


RESEARCH

Open Access



Paracrine activity of *Smurf1*-silenced mesenchymal stem cells enhances bone regeneration and reduces bone loss in postmenopausal osteoporosis

Alberto González-González¹, Itziar Álvarez-Iglesias¹, Daniel García-Sánchez², Monica Dotta¹, Ricardo Reyes³, Ana Alfonso-Fernández⁴, Alfonso Bolado-Carrancio⁶, Patricia Díaz-Rodríguez⁵, María Isabel Pérez-Núñez⁴, José Carlos Rodríguez-Rey¹, Jesús Delgado-Calle² and Flor M. Pérez-Campo^{1*} 

Abstract

Background Osteoporosis (OP), characterized by reduced bone mass and mineral density, is a global metabolic disorder that severely impacts the quality of life in affected individuals. Although current pharmacological treatments are effective, their long-term use is often associated with adverse effects, highlighting the need for safer, more sustainable therapeutic strategies. This study investigates the pro-osteogenic and anti-resorptive potential of the secretome from *Smurf1*-silenced mesenchymal stem cells (MSCs) as a promising cell-free therapy for bone regeneration.

Methods Conditioned media (CM) from *Smurf1*-silenced rat (rCM-*Smurf1*) and human MSCs (hCM-*Smurf1*) was collected and analyzed. Pro-osteogenic potential was assessed by measuring in vitro mineralization in human and rat MSCs cultures. In vivo, studies were conducted using a rat ectopic bone formation model and a post-menopausal osteoporotic mouse model. Additionally, primary human osteoporotic MSCs were preconditioned with hCM-*Smurf1*, and their osteogenic capacity was compared to that induced by BMP2 treatment. Ex vivo, human bone explants were treated with hCM-*Smurf1* to assess anti-resorptive effects. Proteomic analysis of the soluble and vesicular CM fractions identified key proteins involved in bone regeneration.

Results CM from *Smurf1*-silenced MSCs significantly enhanced mineralization in vitro and bone formation in vivo. Preconditioning human osteoporotic MSCs with hCM-*Smurf1* significantly increases in vitro mineralization, with levels comparable to those achieved with BMP2 treatment. Additionally, in ex vivo human bone cultures, treatment with hCM-*Smurf1* significantly reduced RANKL expression without affecting OPG levels, indicating an anti-resorptive effect. In vivo, CM from *Smurf1*-silenced MSCs significantly increased bone formation in a rat ectopic model, and its local administration reduced trabecular bone loss by 50% in a post-menopausal osteoporotic mouse model after a single administration within just four weeks. Proteomic analysis revealed both soluble and vesicular fractions of hCM-*Smurf1* were enriched with proteins essential for ossification and extracellular matrix organization, enhancing osteogenic differentiation.

*Correspondence:

Flor M. Pérez-Campo

f.perezcampo@unican.es

Full list of author information is available at the end of the article



© The Author(s) 2025. **Open Access** This article is licensed under a Creative Commons Attribution-NonCommercial-NoDerivatives 4.0 International License, which permits any non-commercial use, sharing, distribution and reproduction in any medium or format, as long as you give appropriate credit to the original author(s) and the source, provide a link to the Creative Commons licence, and indicate if you modified the licensed material. You do not have permission under this licence to share adapted material derived from this article or parts of it. The images or other third party material in this article are included in the article's Creative Commons licence, unless indicated otherwise in a credit line to the material. If material is not included in the article's Creative Commons licence and your intended use is not permitted by statutory regulation or exceeds the permitted use, you will need to obtain permission directly from the copyright holder. To view a copy of this licence, visit <http://creativecommons.org/licenses/by-nc-nd/4.0/>.

Conclusions The *Smurf1*-silenced MSCs' secretome shows potent osteogenic and anti-resorptive effects, significantly enhancing bone formation and reducing bone loss. This study provides compelling evidence for the therapeutic potential of *Smurf1*-silenced MSC-derived secretome as a non-toxic and targeted treatment for osteoporosis. These findings warrant further in vivo studies and clinical trials to validate its therapeutic efficacy and safety.

Keywords Osteoporosis, *Smurf1*, Secretome, Mesenchymal stem cells

Background

Osteoporosis (OP), a systemic metabolic disease characterized by a decrease in bone mass and Bone Mineral Density (BMD), is recognized as a global public health problem and a heavy socioeconomic burden [1]. Women reach peak BMD in puberty and men somewhat later but, from about 30 years of age, a negative bone balance is observed in both sexes [2]. This bone loss is further accelerated in women during menopause, when estrogen production from the ovaries ceases [3]. It is calculated that a decrease of around 50% of trabecular bone and 30% of cortical bone will then occur during the first ten years after menopause, highly increasing the risk of fragility fractures [4]. According to statistics from the International Osteoporosis Foundation, 1 in 3 women over the age of 50 and 1 in 5 men will experience osteoporotic fractures in their lifetime. Importantly, the incidence of OP as well as that of fragility fractures is set to increase over coming decades as the global population ages, posing challenges to health care systems worldwide.

Pharmacological therapies for OP have important limitations and rare but severe side effects, including, atypical femoral fractures, osteonecrosis of the jaw, strokes and even cancer [5]. These adverse effects are increased when the treatments are used for long periods of time, a major inconvenient in the case of a chronic disease such as OP. Thus, despite recent advances in the field, there is still a clinical need to develop safe and cost-effective treatments for OP that enable long term therapies.

Several preclinical studies have investigated the osteogenic potential of MSCs and their application in the treatment of bone related diseases, such as OP [6–8]. However, the difficulty to scale up the production of MSCs without losing differentiation potential, the possible acquisition of deleterious mutations during long expansion times, leading to potential tumorigenicity, and other safety risks related to stem cell transplantation have hampered the translation of MSCs-based therapies to the clinic. Nevertheless, there is growing evidence indicating that the beneficial effect shown by MSCs upon transplantation is mainly linked to the ability of these cells to secrete a plethora of biomolecules and extracellular vesicles (EVs) with important pro-regenerative, pro-angiogenic and immunomodulatory effects [9–12]. This milieu, known as “secretome”, comprises different

cytokines, chemokines and angiogenic and growth factors, either in a soluble form or carried by EVs. MSCs' secretome exerts its beneficial effects on other resident cells in the bone marrow maintaining a microenvironment that facilitates proper bone homeostasis [13, 14]. The drawbacks linked to cell-based therapies, together with the realization that MSCs paracrine activity is in fact a major player in the regeneration, as seen in various trials involving MSCs, have prompted a change in paradigm [15, 16]. Multiple fundamental studies now support the application of MSCs-derived secretome in tissue regeneration. Bioactive factors secreted by MSCs, such as Osteoprotegerin (OPG) or Bone morphogenetic protein-2 (BMP2) are known to promote healing and tissue repair [17, 18]. Importantly, the plasticity of MSCs' secretome allows for its engineering to suit specific purposes aimed at tissue regeneration. Different approaches have been carried out to develop an MSCs-derived secretome or EVs cargo for improving bone regeneration, from pre-conditioning MSCs with different biochemical compounds, small molecules, or cytokines to subjecting the MSCs to diverse biophysical cues or to directly altering MSCs gene expression through genetic manipulation [19, 20]. Enhancing pro-osteogenic capacity of MSCs' secretome would allow the use of cell-free systems, overcoming the regulatory hurdles linked to the clinical translation of cell-based therapies, favoring the scalability of manufacturing processes and the possibility of producing off-the-shelf options.

We have previously demonstrated that silencing of inhibitors of the main osteogenic pathways using GapmeRs, a particular type of Locked-nucleic Acid Antisense Oligonucleotides, significantly increases the osteogenic potential of MSCs from osteoporotic patients, characterized by an intrinsically reduced osteogenic potential [21, 22]. Although the internalization of the GapmeRs produces only a transient silencing, we have shown that this is enough to prime endogenous MSCs towards osteogenic differentiation leading to a marked increase in bone mineral density in an osteoporotic mouse model [23]. However, while this method only induces transient modifications of the MSCs expression pattern, we cannot fully rule out possible off target effects of the GapmeRs upon translation of this method to the clinic. The development of drugs that would avoid manipulations

of endogenous MSCs would certainly bypass this problem. We hypothesize that the priming process induced by the transient silencing of key osteogenic inhibitors, would trigger important changes in gene expression and protein production, leading to a secretome enriched in pro-osteogenic factors. This shift would likely enhance the presence of pro-osteogenic molecules in the cellular cytoplasm, modifying the protein secretory profile and the cargo of EVs, which could include proteins and nucleic acids, altering the functionality of other cells in the bone microenvironment and thus, influencing bone homeostasis. The highly significant pro-osteogenic effect we observed *in vivo* when *Smurf1*-silenced MSCs were implanted into an ectopic mouse model compared to the results obtained *in vitro* would reinforce the key paracrine role of the secretome of MSCs where this gene has been transiently silenced [24, 25]. This current work investigates this paracrine effect and explores the possible transition to cell-free systems for bone regeneration, with the aim of simplify the therapeutic process and reduce the risk of manipulating endogenous MSCs.

Methods

The work has been reported in line with the ARRIVE guidelines 2.0.

Murine and human primary cell harvesting

Rat Mesenchymal stem cells (rMSCs) were obtained from the bone marrow of two-month-old healthy Sprague–Dawley rats as previously described [26] and cultured for 10–14 days at 37 °C and 5% CO₂ in MesenPRO RS Medium (ThermoFisher Scientific, Waltham, MA, USA) supplemented with GlutaMAX. Only one cell passage was allowed before using the cells to avoid replicative senescence. All animal experiments conducted in this study were reviewed and approved by the Consejería de Agricultura y Ganadería de Cantabria under protocol number PI08/21.

Primary human MSCs (hMSCs) were isolated from the femoral heads of patients who had suffered osteoporotic fractures and required hip replacement surgery, as previously described [27]. Twenty-three women between the ages of 65 and 85 were included in the study, all of whom provided written consent. Patients with cancer, severe chronic disorders, or under the influence of medications known to impact bone metabolism were excluded from the study.

The study was conducted according to the guidelines of the Declaration of Helsinki and approved by the Institutional Bioethics Committee of the University of Cantabria (2022.065).

Cell culture and osteogenic differentiation

The human MSC line ASC52telo (Ref. SCRC4000, ATCC, Manassas, VA, USA) was cultured in Dulbecco's Modified Eagle's Medium (DMEM, Invitrogen, Waltham, MA, USA), supplemented with 10% Fetal Bovine Serum (FBS) (ThermoFisher Scientific, Waltham, MA, USA) and 1% penicillin–streptomycin (ThermoFisher Scientific, Waltham, MA, USA). Maintenance of this cell line requires supplementation with geneticin (0.2 mg/ml) (G418 Sulphate, Corning, Manassas, USA). For osteogenic differentiation, 20,000 cells/cm² were seeded in a 24 well plate and incubated overnight to allow attachment. Osteogenic induction was achieved by replacing the culture medium with osteogenic medium. For rMSCs and hMSCs, the osteogenic media consisted of DMEM supplemented with 20 mM β-glycerophosphate, 50 μM ascorbic acid and 1 μM dexamethasone. For ASC52telo, DMEM was supplemented with 2 mM β-glycerophosphate, 50 μM ascorbic acid and 0.1 μM dexamethasone. Differentiation was allowed to progress for up to 12 days.

Cell transfection

All GapmeRs used in this study were purchased from Exiqon (Qiagen, Vnlo, The Netherlands). GapmeRs were acquired for silencing of *Smurf1* in rat primary cells (3,688,232 LG00220909-DDA) and of human *SMURF1* in the ASC52telo cell line (Ref. 3,633,952 LG00783776-DDA). An Antisense LNA GapmeR Negative Control A (Ref. 339,516) was used as a negative control in all the experiments. Lipofection was performed using Dharmafect (Dharmacon, Horizon Discovery, Cambridge, UK) as previously described [22]. For transfection, rMSCs and the ASC52telo cells were seeded at 20,000 cells/cm² and 15,000 cells/cm² respectively. Two hours before transfection, culture medium was replaced by Opti-MEM I medium (Invitrogen, Waltham, Massachusetts, USA). Twenty-four hours after transfection, one volume of DMEM with 10% FBS and 1% penicillin–streptomycin was added to the wells. Cells were further incubated at 37 °C for another 24 h. Forty-eight hours after transfection, cells were washed once with PBS and fresh complete culture medium was added.

To test GapmeR delivery efficiency we used an Antisense LNA GapmeR Negative Control A labeled with fluorescein (Ref. 339,515 LG00000002-DDA). We used flow cytometry to confirm GapmeR uptake in the cells. A FACSCanto II flow cytometer with FASCDiva Software (BD Bioscience, San Diego, CA, USA) was used to carry out this analysis.

Quantitative RT-qPCR analysis

mRNA was isolated from cell cultures, after washing the cells twice with PBS and collecting them with TRIzol reagent (Invitrogen, Waltham, MA, USA) by scraping the plate surface. mRNA extraction was performed following the TRIzol manufacturer's protocol. Between 1 and 1.5 µg of RNA were isolated from a confluent well in a 24-well plate. Gene expression analysis was carried out by real-time qPCR. RNA was extracted from cell cultures, and cDNA conversion was performed as previously described [22]. Taqman assays were used for this analysis (ThermoFisher Scientific). Rat probes were: *Gapdh* (Rn01775763_g1), *Smurf1* (Rn01412801_m1), *Runx2* (Rn01512298_m1), *Alpl* (Rn01516028_m1), *Bglap* (Rn00566386_g1). Likewise, human assays probes were as follows: *GAPDH* (Hs99999905_m1), *SMURF1* (Hs00410929_m1), *RUNX2* (Hs00231692_m1), *ALPL* (Hs00758162_m1), *BGLAP* (Hs01587814_g1), *PRELP* (Hs01941580_s1), *FMOD* (Hs05021078_s1), *CCN2* (Hs00170014_m1), *SPARC* (Hs00234160_m1).

Conditioned media production

Forty-eight hours after transfection, the cells were thoroughly washed with PBS and 0.2 ml/cm² of MesenPRO RS Medium with Glutamax (no supplements) was added to the plates. After a 48 h incubation at 37 °C and 5% CO₂, the conditioned media (CM) was collected. Two successive centrifugations (400 g for 10 min at 4 °C and 1000 g for 10 min at 4 °C) were performed to exclude cellular debris. Finally, the CM was filtered through 0.22 µm filters and stored at −80 °C until needed.

Alkaline phosphatase activity

Cells undergoing osteogenic differentiation were washed twice with PBS and then collected by scrapping in 0.05% Triton X-100 (Merck KGaA, Darmstadt, Germany) to lysate the cells. Samples underwent 3 cycles (30"on/30" off) of sonication at 4 °C and centrifuged to collect the supernatant. Finally, samples were stored at −80 °C until needed. Alkaline Phosphatase enzymatic activity was quantified as previously stated [28]. Absorbance was measured using an Eon Microplate Spectrophotometer (BioTek, Winooski, VT, USA).

Mineral deposition staining and quantification

To evaluate mineralization, calcium deposition was assessed via Alizarin Red staining. The staining and subsequent quantification was conducted using a modified version of a previously documented procedure [29]. Briefly, cell monolayers were fixed using ethanol 70% for 1 h. Then, cells were washed three times with distilled water and Alizarin Red S staining solution was added for 10 min at RT. After three more washes with distilled

water, monolayers were left to dry. Alizarin Red Quantification was performed as recently described [30]. Eon Microplate Spectrophotometer was used for absorbance detection at 405 nm (BioTek, Winooski, VT, USA).

Proliferation assessment

A colorimetric MTT (3-(4,5-dimethylthiazol-2-yl)-2,5-diphenyltetrazolium bromide) assay was used to analyse cell proliferation. Cells were seeded after 48 h-exposure to secretome, and culture medium was changed to DMEM with 0.5 mg/ml of MTT at days 1, 3, 5, 7, and 9. After 4 h of incubation at 37 °C, the medium was discarded and 100 µL of 2-propanol were added for another 10 min at 37 °C incubation on agitation. Absorbance was measured at 570 nm (BioTek, Winooski, VT, USA).

Cell migration assay

To assess cell migration capability, a wound healing assay was conducted. Cells were seeded at high density in 6-well plates (25,000 cells/cm²) and transfected according to the previously described protocol. Forty-eight hours post-transfection, MesenPro medium was introduced, and 400 µm-wide wounds were created in each plate. Photographs were captured at 3-h intervals over a 72-h period. For each sample, six different regions along the wound were documented and analyzed. The wound area was measured every 12 h. ImageJ 1.53 software was used to analyze the images, allowing for the evaluation of wound size through the quantification of the empty areas within the lesion.

Chemotactic assay

Chemotactic assays were performed using Transwell Permeable Support Inserts with an 8.0 µm pore size (Corning, Somerville, Massachusetts, USA). Cells were seeded on the upper side of the insert and incubated overnight at 37 °C to allow attachment. Subsequently, conditioned media were added to the lower chamber, and the cells were returned to the incubator for 24 h. Both sides of the insert were then carefully washed with PBS, and 100% methanol was added to fix and permeabilize the cells. The cells were stained with crystal violet, and the upper side of the inserts was carefully cleaned with a cotton swab to remove non-migrant cells. After staining, cells that had migrated to the lower part of the insert were counted using a Zeiss Axiovert 200 Microscope (Zeiss, Jena, Germany) and ImageJ 1.53c software.

Ex vivo human bone culture

For establishing ex vivo bone culture, we collected and culture trabecular bone cylinders of the central part of human femoral head samples using a trephine. The cylinders were processed as previously described [31]. In brief,

bone cylinders, 5 mm Ø were cut in smaller fragments of approximately 4–5 mm height, washed with PBS and cultured in 50% secretome for 4 days. In day 2, half of the culture medium was collected and changed for fresh one. Bone pieces were washed with PBS, immersed in TRIzol, and disaggregated for subsequent gene expression analyses. Samples were obtained from 3 women with no conditions or medications that may alter bone metabolism.

In vivo ectopic model

A rat ectopic model was used for the analysis of the osteogenic capacity *in vivo*. This model consisted of using scaffolds with cells and secretome on 2 months-old healthy Sprague–Dawley rats. Secretome was produced as previously described and concentrated 10X using Amicon Ultra-15 centrifugal filter units (Sigma Aldrich, San Luis, Missouri, USA). Then, 80,000 rMSCs were resuspended in 100 µl of secretome and this mixture was load onto 4 mm diameter alginate scaffolds. Scaffolds were incubated at 37 °C overnight to allow cell attachment. Subsequently, scaffolds were imbedded intradermally in the back of the animals under isoflurane anaesthesia. Scaffolds remained in the animals for 8 weeks. Analgesia was maintained for 2 days after the procedure. All animals carried controls scaffolds. The other experimental conditions were randomly allocated to the different animals, so we end up with three different scaffolds per condition. After this time, all scaffolds were extracted and processed for histological analysis. Euthanasia of Sprague–Dawley rats was performed by CO₂ inhalation. All animals used in this experiment were housed in the University of Cantabria's Animal Housing and Experimentation Service for the duration of the experiment.

Histological analysis

The implants retrieved from the rats were preserved in 10% formaldehyde for 6 h and subsequently decalcified in 20% EDTA in PBS (pH 7.4) for one week at 4 °C, with the solution being changed twice weekly. After decalcification, the implants were embedded in paraffin, sectioned into 5-micron slices, deparaffinized, and stained using standard protocols. Masson–Goldner Trichrome staining was used for collagen detection. For the indirect immune-enzymatic technique, the deparaffinized and rehydrated sections in Tris buffered saline (TBS) (pH 7.4) were subjected to antigen retrieval in citrate buffer (pH 6) for 5 min at 90 °C and then blocked in a solution of 2% FBS in 0.2% TBS-Triton. To study osteogenic differentiation the sections were incubated overnight at 4 °C with polyclonal anti-osteocalcin (OCN) antiserum (1:100) and polyclonal anti-ALPL antiserum (1:100) in blocking buffer. After washing with TBS, the sections were incubated with a donkey anti-rabbit IgG antibody conjugated

with biotin (1:500) for 60 min, followed by streptavidin-peroxidase (1:500) for another 60 min. Peroxidase activity was visualized using 0.005% 3,3'-diaminobenzidine and 0.01% hydrogen peroxide in Tris–HCl buffer (0.05 M, pH 7.6). The specificity of immunostaining was verified by replacing the primary antibodies with normal serum. OCN and ALPL stainings were quantified by applying a fixed threshold to select for positive staining within the implant region, with the positive pixel areas normalized to those measured from the control group and reported as relative staining intensities. Additionally, the reported values were adjusted to account for baseline background signal, as determined from negative control samples, ensuring accurate representation of specific staining.

In vivo post-menopausal osteoporotic model

Four-month-old female CD1 mice were used in this procedure. Mice underwent dorsal ovariectomy (OVX) ($n=12$) or were subjected to the same surgical procedure without removing the ovaries (NO-OVX group, $n=4$). One week after, the OVX mice were randomly allocated into 3 groups (4 mice/group). With all the mice under isoflurane anesthesia, each of the groups received an injection of 5 µl of NaCl (NaCl group), or 5 µl of 50X concentrated conditioned media (CM-Ctrl or CM-*Smurf1* groups) administered directly into the femur medullary cavity. Analgesia was maintained for two days after the procedure. Four weeks later mice were sacrificed, and femurs were extracted and fixed. Before tissue procurement, mice were injected with an overdose of ketamine (180 mg/kg) + xylazine (30 mg/kg) for humane euthanasia. Subsequently, bones were scanned by micro-computed tomography (microCT) using Scanco vivaCT 80 (Scanco Medical, Brüttisellen, Switzerland) and bone architecture was measured. These procedures were approved by the Animal Care Committee at the University of Cantabria. All animals used in this experiment were housed in the University of Cantabria's Animal Housing and Experimentation Service for the duration of the experiment.

Exosomes purification, characterization, and functionality assays

Exosome purification was carried out by serial centrifugations at increasing speeds, following manufacturer's instructions of the ExoStep Kit (ImmunoStep, Salamanca, Spain). Once isolated from the CM, CD63 and CD9 exosome markers were identified by flow cytometry on A FACSCanto II flow cytometer with FASCDiva Software. Exosomes were characterized in terms of average diameter, polydispersity index (Pdl), and zeta-potential (ζ -potential) by dynamic light scattering using a Zetasizer Nano (Malvern). All measurements were made

in triplicate. Morphological characterization by transmission electron microscopy (TEM) was performed using 10 μ L samples that were deposited on carbon membrane coated copper grids and stained with a 2% w/v phosphotungstic acid solution for 2 min prior imaging.

To evaluate exosomes functionality, human ASC52telo MSCs were cultured in Nunc Lab-Tek Chamber Slides (ThermoFisher Scientific) at 15,000 cells/cm² and were allowed to attach overnight. Exosomes were stained with Vybrant CM-DiI Cell-Labeling Solution (ThermoFisher Scientific) following manufacturer instructions. Stained exosomes were resuspended in DMEM with 10% FBS and 1% penicillin–streptomycin and added to the cells for 2 h. Cell uptake of stained exosomes was recorded using Nikon Eclipse Ti. After this time, cells were washed with PBS, fixed with paraformaldehyde 3.7% (ThermoFisher Scientific), permeabilized using 0.5% Triton X-100 and labeled with phalloidin dye conjugate (ab176753; Abcam, Cambridge, Great Britain) to show cell cytoskeleton. Nikon A1R-HD TIRF Confocal Microscope (Nikon Instruments Inc) and ImageJ 1.53c software were used to verify the cell uptake.

Mass spectrometry

The conditioned media (CM) was produced as stated in the “Conditioned Media Production Section”. Twelve ml of CM produced for 48 h incubation of cells previously transfected with Ctrl or *SMURF1* GapmeRs were centrifuged at 1,000 rpm for 5 min at 4 °C, followed by a second centrifugation at 3,000 rpm for 10 min at 4 °C. The exosomal fraction was then isolated using ultracentrifugation at 100,000 rpm for 1 h at 4 °C in a Beckman Optima L90-k ultracentrifuge. The resulting supernatant was labeled as the soluble fraction, and the pellet was designated as the exosomal fraction. The soluble fraction was concentrated using Amicon Ultra 10 kDa centrifugal filters. Both fractions underwent mass spectrometry analysis following an in-solution digest protocol. Briefly, proteins were denatured with 6 M guanidine hydrochloride, reduced, and alkylated with 5 mM TCEP and 10 mM chloroacetamide, and sequentially digested with MS-grade Lys-C and trypsin. Peptides were desalted and purified, as described in prior protocols. The eluted peptides were lyophilized, resuspended in 0.1% TFA, and analyzed using LC–MS/MS on an Orbitrap Fusion™ Lumos™ Tribrid™ Mass Spectrometer. Protein identification and quantification were carried out using the DIA-N/N software and Perseus software, with normalization to the total protein in the cell culture. Statistical significance was determined using an adjusted t-test against control CM, with a *p*-value threshold of 0.05 and a fold change of 2 or greater.

Statistical analysis

Error bars on graphs represent the standard error of the mean values. Depending on sample size, statistical significance was calculated using the Students' *t*-test (for $n > 5$) or the Mann–Whitney U test (for $n = 3$). To assay the bone formation in the mouse ectopic model, statistical analysis was performed with SPSS.25 software by means of a one-way analysis of variance (ANOVA) with a Tukey multiple comparison post-test. Significance was set at $p < 0.05$.

Results

In vivo and in vitro MSCs' osteogenesis is augmented by conditioned media from *Smurf1*-deficient rat mesenchymal stem cells

We have previously established conditions for the efficient silencing of *Smurf1* expression in rat mesenchymal stem cells (rMSCs) using a specific GapmeR and have demonstrated that this silencing significantly increases the osteogenic potential of MSCs in vivo in both a calvaria and an ectopic mouse model [24, 25]. However, the ability of these cells to directly undergo osteogenic differentiation upon *Smurf1* silencing in vitro is not as evident, suggesting a key role of their paracrine activity in vivo. To test the hypothesis that the secretome of *Smurf1*-silenced MSCs possesses a substantial osteogenic potential, we investigated whether conditioned media (CM) from primary rMSCs with silenced *Smurf1* (rCM-*Smurf1*) could enhance osteogenic differentiation both in vitro and in vivo. The following experiments were designed to investigate the concept of MSC-to-MSC communication, where the secretome of *Smurf1*-silenced MSCs may influence the osteogenic differentiation of other MSC populations, highlighting their potential to modulate the local microenvironment through paracrine mechanisms. For this purpose, rMSCs were treated with rCM-*Smurf1* and CM of rMSCs transfected with a control GapmeR (rCM-Ctrl), for 48 h prior to the induction of osteogenic differentiation for 12 days. We hypothesize that the secretome acts primarily during the initiation stages of osteogenic differentiation, triggering or accelerating the process. This hypothesis is supported by the secretome's ability to deliver bioactive molecules which prime cells for differentiation by modulating key signalling pathways. Given this rationale, we focused on early markers of osteogenesis, such as *Runx2* and *Alpl*, to assess the initial phases of the differentiation process. Our results indicate a minor increase of the key osteogenic transcription factor *Runx2* (Runt related factor 2) expression at day 8 of differentiation in rMSCs treated with rCM-*Smurf1* compared to those treated with CM-Ctrl, although this increase was not statistically significant. Nonetheless, we observed that, at days 8 and 12, Alkaline phosphatase

(*Alpl*) expression levels were significantly increased in cells treated with rCM-*Smurf1*, suggesting an enhanced osteogenic differentiation under this condition (Fig. 1A, top panel). This idea was further supported by a significant rise in the ALPL activity in cells preconditioned with rCM-*Smurf1* (378% higher than cells treated with CM-Ctrl) and the observation that mineralization levels, as measured by Alizarin Red staining, were also significantly higher (85%) in these cells compared to those pretreated with rCM-Ctrl (Figs. 1A bottom panel and B).

Additionally, to analyze the *in vivo* pro-osteogenic capacity of the rCM-*Smurf1*, rMSC were seeded in alginate scaffolds and pre-treated with rCM-*Smurf1* and rCM-Ctrl for 16 h before being ectopically implanted in a subcutaneous location in Sprague–Dawley rats, as previously described [22] (Fig. 1B). This ectopic model enables the specific assessment of the transplanted cells' contribution to bone tissue formation in the scaffold. In accordance with current guidelines for the use of experimental animals, and to reduce the number of rats used, we performed up to six implants into a single rat [22]. As controls, an empty scaffold (No Cells) and a scaffold seeded with untreated MSCs were used. The implants were surgically removed after 8 weeks, and the extent of new bone formation was analyzed by histological techniques. An average of three scaffolds for condition were analyzed in these experiments. Bone matrix was particularly abundant in scaffolds seeded with rMSCs pretreated with rCM-*Smurf1*, as shown by extensive areas of collagen-stained dark blue color with the Masson–Goldner technique (Fig. 1C). Cells embedded within the matrix and surrounded by an empty region, resembling osteocytes within osteocytic lacunae, were observed in the rCM-*Smurf1* sample at higher magnification. Quantification of new bone formation clearly indicates a significantly higher presence of bone matrix in the rCM-*Smurf1* scaffolds. Furthermore, immunohistochemistry analysis with anti-alkaline phosphatase (ALPL) and anti-osteocalcin (OCN) antibodies demonstrated that scaffolds seeded

with cells pre-treated with the rCM-*Smurf1* exhibited significantly higher levels of these osteogenic proteins compared to those seeded with cells pre-conditioned with rCM-Ctrl.

***Smurf1*-silenced hMSC-conditioned media acts as an inductive agent for osteogenic differentiation in human osteoporotic MSCs**

The utilization of a human cell line to generate a pro-osteogenic conditioned media (CM) would significantly streamline the production process for a secretome-based biomedical product on an industrial scale. Given that the long-term aim of this project is the development of such product for human application, we investigated whether the effects observed on primary rMSCs could be replicated in a human MSCs cell line. To achieve this, we first selected a GapmeR capable of inducing an adequate silencing of *SMURF1* in the human MSC line ASC52telo. By using a GapmeR concentration of 20 nM we were able to systematically achieve a silencing of *SMURF1* expression $\geq 80\%$ (Supplementary Fig. 1). Following the establishment of these silencing conditions, we evaluated the osteogenic potential of conditioned media (CM) derived from *SMURF1*-silenced ASC52telo (hCM-*SMURF1*) and a control CM also produced in the ASC52telo cell line (hCM-Ctrl). We found a clear trend towards an increase in the expression of Alkaline phosphatase (*ALPL*), one of the main osteogenic markers, in ASC52telo cells pretreated with the hCM-*SMURF1*, although this increase was not significant (Supplementary Fig. 2). Similar results were found when ALPL enzymatic activity was measured in the same samples (Supplementary Fig. 2). However, the significantly higher levels of mineralization obtained by the incubation of the ASC52telo cells with the hCM-*SMURF1* compared to those obtained after the incubation with hCM-Ctrl, would indicate a positive effect on this process of the hCM-*SMURF1*, underscoring the biological relevance of our findings (Supplementary Fig. 2).

(See figure on next page.)

Fig. 1 *In vitro* and *in vivo* analysis of rMSCs-CM pro-osteogenic potential. **(A)** Top panel. Relative expression levels of osteogenic markers (*Runx2* and *Alpl*) in primary rat MSCs were assessed using semi-quantitative PCR after 48-h of pre-treatment with either rCM-*Smurf1* or rCM-Ctrl. Bottom panel. Left graph illustrates the alkaline phosphatase (AP) activity in rMSCs cells preconditioned with rCM-*Smurf1* or rCM-Ctrl. Quantification of *in vitro* mineralization is shown in the bottom panel, right part, of the figure. **(B)** Alizarin Red staining measuring mineralization was performed every four days during osteogenic differentiation. The images display results from representative samples. For all graphs, results are presented as means \pm SEM. ($n = 3$) with each sample analyzed in technical triplicates. **(C)** Masson's trichrome staining of ectodermally implanted scaffolds 8 weeks after implantation. Images show histological analysis of sections obtained from decalcified implants. Collagen of the extracellular bone matrix stained in dark blue. White arrowheads indicate osteocytes-like cells surrounded by lacunae and immersed in the mineralized matrix (Magnification $\times 4$). A higher magnification shows osteocyte cells surrounded by osteocytic lacunae in CM-*Smurf1* (Magnification $\times 9$). Histological sections of the ectodermic scaffolds stained by immunohistochemistry with specific antibody for ALPL and OCN (Magnification $\times 4$). Graphs show the quantification of new bone formation and ALPL and OCN levels observed in the histological sections. Results are presented as means \pm SEM. * p -value < 0.05 ; ** p -value < 0.01 ; *** p -value < 0.001 . ($n = 3$)

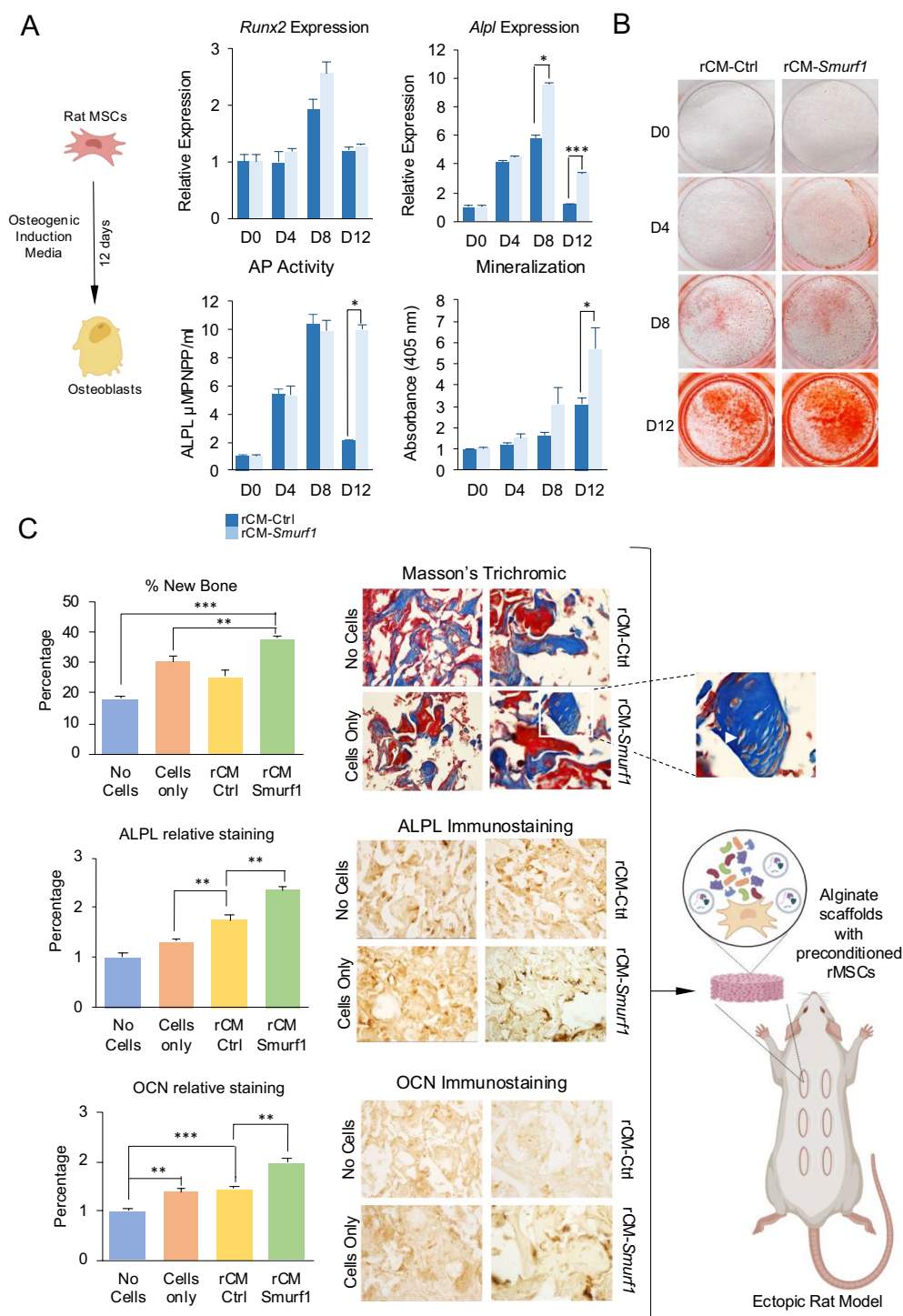


Fig. 1 (See legend on previous page.)

In previous works, we demonstrated that bone marrow MSCs from osteoporotic patients (hMSCs-OP) exhibit a markedly diminished osteogenic potential relative to those derived from healthy donors [27]. To in vitro assess the suitability of CM-SMURF1 as a

potential pro-osteogenic therapeutic agent, it was essential to ascertain its efficacy in enhancing the osteogenic differentiation of hMSCs-OP. Hence, we produced the CM in the human MSC cell line ASC52telo transfected with the SMURF1 or Ctrl GapmeRs, using the same

procedure as previously described. The pro-osteogenic capacity of these two CMs (hCM-*SMURF* o hCM-Ctrl) was then evaluated by pre-treating hMSCs-OP previously isolated from the femoral heads of osteoporotic patients, with these two CM for 48 h before initiating osteogenic differentiation (Fig. 2). The analysis was individually performed in a total of twenty-three MSCs primary cultures, each of them obtained from an individual of a cohort of osteoporotic female patients who met our stringent inclusion criteria. The analysis at day 20 of osteogenic differentiation revealed no significant differences in the expression levels of principal osteogenic genes *RUNX2* and *ALPL*. Nonetheless, a clear tendency towards an increase in *ALPL* expression was observed in hMSCs-OP pre-conditioned with hCM-*SMURF1* (Fig. 2A, top panel). Importantly, significant differences in both the alkaline phosphatase activity and the mineralization degree of hMSCs-OP pre-treated with the hCM-*SMURF1* were clearly observed across all experiments performed (Fig. 2A bottom panel and Fig. 2B). Moreover, comparison of the levels of ALPL activity and mineralization induced by the treatment with the hCM-*SMURF1* were highly similar to those observed upon treatment of the primary cells with bone morphogenetic protein 2 (BMP2), a known inducer of bone formation commonly used in the clinic (Fig. 2A).

To gain insight into how hCM-*SMURF1* affects bone formation within the context of bone's natural microenvironment, we used human ex vivo bone cultures from the femoral head of three osteoporotic patients. A total of six bone samples per patient were cultured in an appropriate media in the presence of hCM-*SMURF1* or hCM-Ctrl as explained in the material and methods section. Bone fragments were maintained in culture for 4 days with 50% CM. After this time, bone fragments were disaggregated, and the total mRNA extracted to quantify the gene expression of key markers of bone homeostasis. Interestingly, the CM from MSCs transfected with the *SMURF1* GapmeR showed a significant decrease in the expression levels of the Receptor Activator of Nuclear Factor Kappa B Ligand (*RANKL*), a key molecule that promotes osteoclasts differentiation and activation, leading to bone resorption (Fig. 2C, top panel). Expression levels of Osteoprotegerin (OPG), which acts as a decoy receptor for RANKL, were however unchanged, leading to an overall reduction of the *RANKL/OPG* ratio (Fig. 2B, bottom panel). This ratio reflects the balance between bone resorption and formation, with a higher ratio indicating increased osteoclast activity and potential bone loss, while a lower ratio suggests reduced bone resorption and potential bone preservation. No significant changes were however observed in the levels of *M-CSF* (Macrophage Colony-Stimulating Factor) and *BGLAP*

(Bone Gamma-Carboxyglutamate protein) (Fig. 2C, bottom panel).

Biosafety of CM-*SMURF1* and effect on basic cellular functions

We conducted a series of assays using the ASC52telo cell line to gain further insight into the biosafety of the CM produced and to investigate its possible impact on fundamental cell functions. Initially, we assessed the influence of CM from hMSCs where *SMURF1* has been silenced on cell proliferation by performing an MTT assay over a period of nine days. Our findings indicate a modest, yet statistically significant increase in cell proliferation in those cells treated with the hCM-*SMURF1* at day seven, however this proliferative effect did not persist at later time points (Fig. 3A). Cell proliferation data are expressed as ratios of absorbance between consecutive days (e.g., Day 5/Day 3, Day 7/Day 5), providing an analysis of relative growth dynamics rather than absolute cell numbers.

Subsequently, we sought to ascertain the capacity of hCM-*SMURF1* to facilitate cellular repair following mechanical damage in a wound healing assay (Fig. 3B). After introducing a defect into a monolayer culture of cells treated with the different CMs, the recovery was monitored at 0, 12, 24 and 36 h until the surface of the plate was fully covered by confluent cells. We observed an overall improvement of the migratory capacity in cells incubated with CM, however, our results showed no significant differences between the control CM and that of hMSCs where *SMURF1* has been silenced.

To investigate the effect of the different CMs on basic properties of MSCs, we investigated whether incubation with CM-*SMURF1* could affect the chemotactic response of MSCs. For this experiment, we employed Stromal cell Derived Factor 1-alpha (SDF1- α) as a benchmark chemotactant to evaluate chemotactic responses in MSCs. In comparison to a baseline of unconditioned media, both CM-Ctrl and CM-*SMURF1* demonstrated a significantly greater capacity to attract hMSCs (Fig. 3C) than that of the control cells growing in the absence of CM. We also noted a significantly higher rate of cell migration towards hCM-*SMURF1*, which greater values to those of the control CM.

Isolation and characterization of the vesicular fraction from the CMs

To efficiently isolate the extracellular vesicles (EVs) from both hCM-*SMURF1* and hCM-Ctrl samples, and to obtain the EV-depleted counterparts, a serial centrifugation protocol was followed according to the guidelines of the International Society of Extracellular Vesicles (ISEV). Nanoparticle Tracking Analysis (NTA)

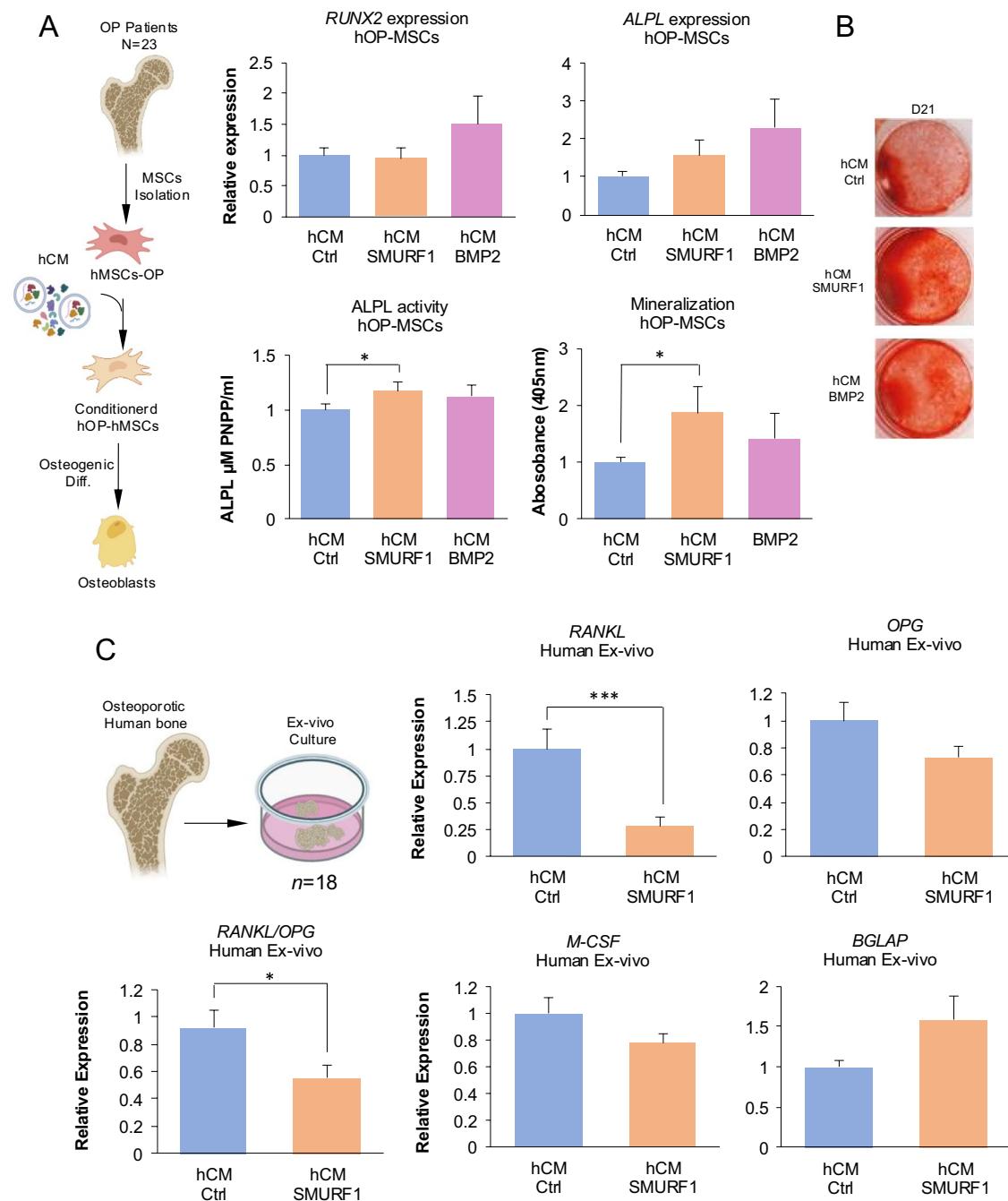


Fig. 2 Pro-osteogenic effect of hCM-SMURF1 on MSCs and bone samples from osteoporotic patients. **(A)** Top panel. In vitro osteogenic potential of primary human MSCs isolated from the femoral head of osteoporotic patients preconditioned with CM-Ctrl, CM-SMURF1 or BMP2. Normalized results of a quantitative PCR measuring the expression of key osteogenic markers *RUNX2*, *ALPL*. Bottom panel left. Graphical representation of the activity of the alkaline phosphatase enzyme. Bottom panel right. Quantification of Alizarin Red staining. Results are presented as means \pm SEM (n = 23). *: p-value < 0.05; ***: p-value < 0.001. **(B)** Alizarin Red staining of representative samples. All analysis were performed after at 20 days of osteogenic differentiation. **(C)** Gene expression analysis of *RANKL*, *OPG*, *M-CSF* and *BGLAP* in human osteoporotic bone samples cultured ex vivo in 50% of CM-CTRL or CM-SMURF1 for 4 days measured by qPCR. Results are presented as means \pm SEM. *: p-value < 0.05; **: p-value < 0.01; *** p-value < 0.001. (n = 18)

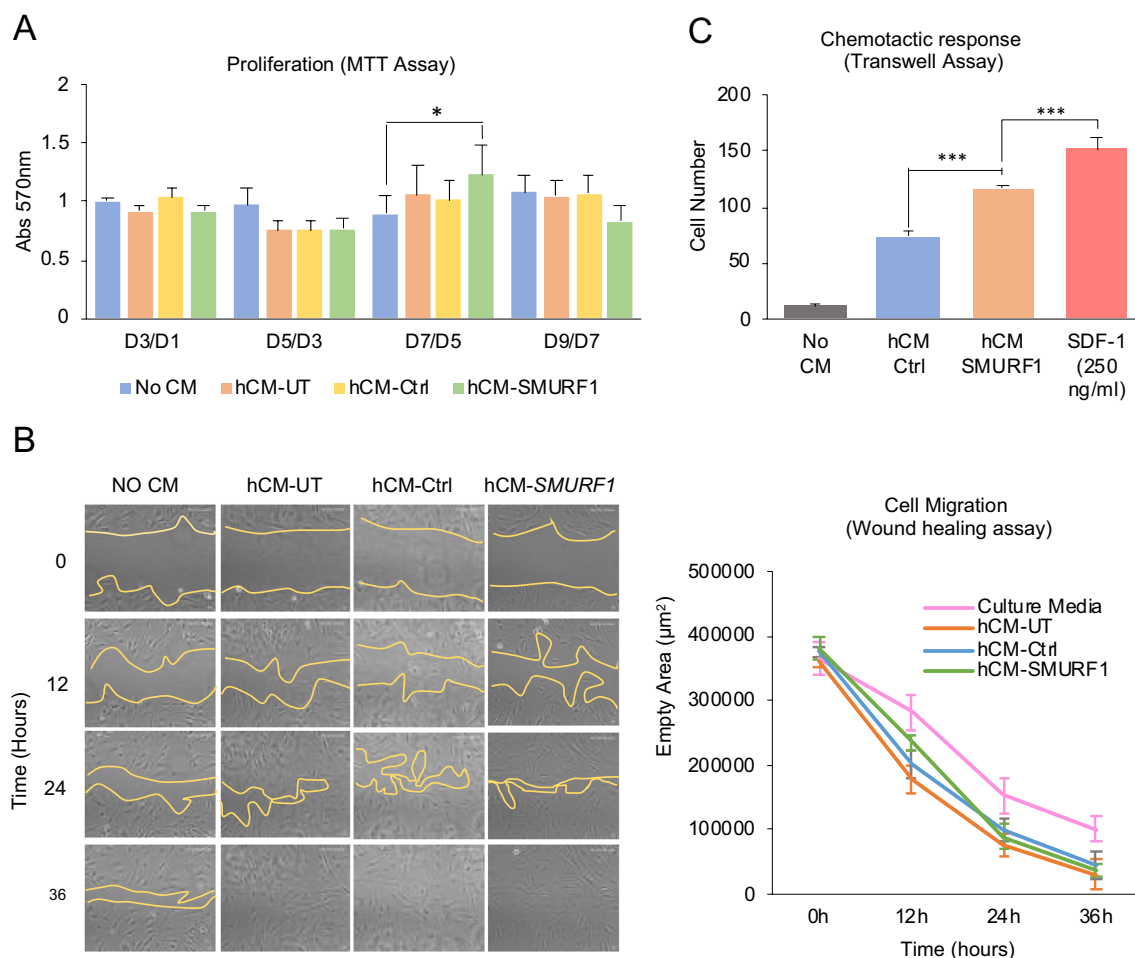


Fig. 3 Analysis of the hCM-SMURF1 effects on basic cellular functions. **(A)** Results from the MTT [3-(4,5-dimethylthiazol-2-yl)-2,5-diphenyltetrazolium bromide] proliferation assay performed during 9 days after 48 h of exposition to normal culture media or to the different CMs (hCM-UT=CM from un-transfected cells). The results are presented as ratios of MTT absorbance between consecutive days. *: p -value < 0.05. ($n=3$) **(B)** Wound healing studying the influence of the different CM on cell migration. Quantification of empty area using ImageJ image processor confirmed the absence of significant changes. Graph represents the average area in five different time-points for each of the experimental conditions. Bars represent the SEM. **(C)** Chemotactic response of MSCs to the different conditioned media was measured using transwell inserts. Media with SDF-1 α was used as a positive control. For all experiments, graph represents the average values of five or three experiments, as indicated. Bars show standard deviation of the mean values. *: p -value < 0.05; **: p -value < 0.01; ***: p -value < 0.001

was used to determine the total particle number and the average size of the isolated EVs. The average particle diameter of the EVs in the fractionated secretome was 131.3 ± 3.7 nm for the CM-Ctrl and 114.3 ± 6 nm for the CM-SMURF1 (Fig. 4A). This indicates the presence of nanometer-sized vesicles in both preparations. The prominent peaks being in the 50–150 nm range suggest the presence of exosomes, which typically range from 30 to 50 nm in size. Transmission Electron Microscopy (TEM) further confirmed the presence of EVs in both samples showing typical vesicular structures in the non-soluble fraction of the secretome

(Fig. 4B). To further characterize the isolated exosomes, an immunobead assay was conducted using a bead-bound capture antibody and fluorochrome-conjugated detection antibody. Flow cytometry analysis confirmed that exosomes from both CM-Ctrl and CM-SMURF1 expressed specific markers CD63 and CD9 on their surface (Fig. 4C).

Staining of EVs with Vybrant CM-Dil verified successful internalization of isolated exosomes by MSCs. High-resolution 3D images of ASC57telo cells incubated with labelled exosomes for 2 h were recorded using live cell confocal microscopy (Fig. 4D and Supplementary Videos 1 and 2).

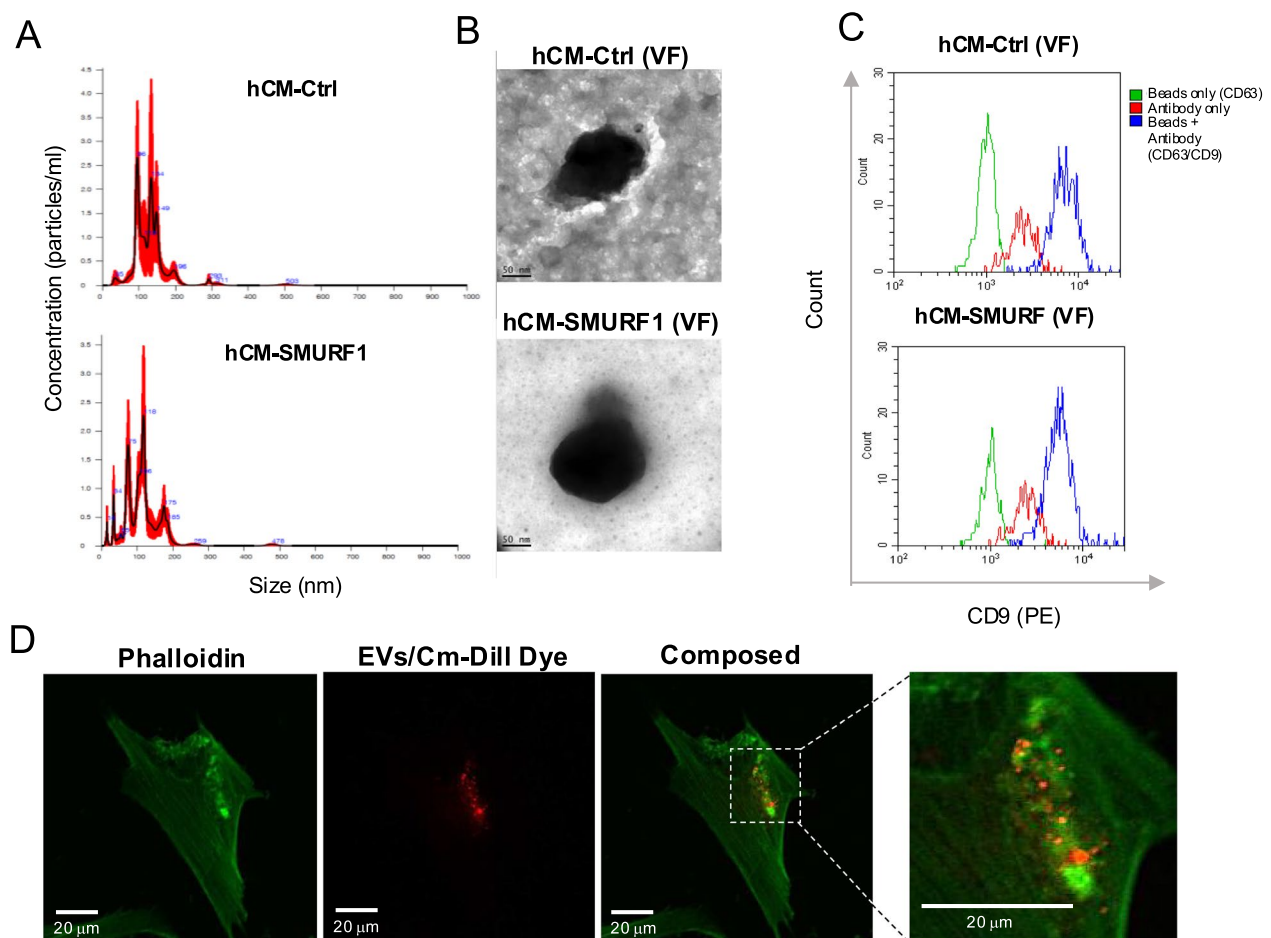


Fig. 4 Characterization of the vesicular fractions isolated from CM-Ctrl and CM-SMURF1. **(A)** Nanoparticle Tracking Analysis (NTA) showing particle size distribution of isolated EVs **(B)** Transmission Electronic Microscopy (TEM) image of EVs isolated from CM-Ctrl and CM-SMURF1. Scale bar 50 nm. **(C)** Flow cytometry analysis using a bead-bound capture antibody system for the detection extracellular vesicle (EVs) markers. CD63 and CD9. **(D)** Confocal microscopy images shown EV stained with Vybrant CM Dil (red) and MSCs stained with Phalloidin (green) after two hours of exposition of cells to the stained EVs. Images obtained were composed by ImageJ

Analysis of the pro-osteogenic activity of the soluble and vesicular fractions of CM-SMURF1

Upon establishing the protocol for isolating the soluble (SF) and vesicular fractions (VF) from hCM-Ctrl and hCM-SMURF1 we investigated their individual capabilities to induce osteogenic differentiation. Prior to osteogenic induction ASC52telo cells were incubated with either the soluble or vesicular fraction derived from CM-Ctrl or CM-SMURF1 for 48 h, following the same protocol already established for the unfractionated CM. Subsequently, the media was replaced, and osteogenic differentiation proceed as per the standard protocol.

Analysis of osteogenic markers on day 16 post-induction revealed a significant increase in the *RUNX2* expression in cells pre-treated with the SF. This also applies to *ALPL* expression, which was mirrored by an enhanced alkaline phosphatase activity in the SF of CM-SMURF1

compared to that of the CM-Ctrl (Fig. 5A). Although no substantial changes in the aforementioned parameters were detected when compared the vesicular fractions of CM-Ctrl and CM-SMURF1, significantly higher degrees of mineralization, quantified via alizarin red staining, were evident between the CM-Ctrl and the CM-SMURF1 in both the soluble and vesicular fractions, which might reflect a contributory role of both fractions in the mineralization process in vitro (Fig. 5A and B).

We next sought to identify proteins that were differentially regulated in the soluble and vesicular fractions of hCM-SMURF1 and hCM-Ctrl. For that, we compared the proteomes of the soluble and vesicular fractions of CM-Ctrl and CM-SMURF1 from four independent silencing experiments by mass spectrometry. The study identified several affected proteins in both the soluble and vesicular fractions (Fig. 5C and Supplementary

Information_Tables 1 and 2). Volcano plots showing differently expressed proteins between hCM-Ctrl and hCM-SMURF1 for both SF and VF (Supplementary Figs. 3 and 4 respectively). Statistical significance was determined using an adjusted *t*-test against CM-Ctrl, with a *p*-value threshold of 0.05 and a fold change of 2 or greater. Among these proteins, we identified key regulators of bone formation, *PREPL* (Prolyl Endopeptidase Like) and *FMOD* (Fibromodulin) overrepresented in the soluble fraction of CM-SMURF1, whereas *SPARC* (Secreted Protein Acidic And Cysteine Rich) and *CCN2* (Cellular Communication Network Factor 2) were overrepresented in the vesicular fraction of CM-SMURF1. In all cases, the validation by qPCR of the MS results agreed with the relative abundance of those proteins found in the MS analysis (Fig. 5D).

To have an overview of the principal processes associated with the proteins which levels were significantly different in the two sets of samples, we performed Gene Ontology (GO) analysis (Supplementary Fig. 5). Significantly enriched proteins from the CM-SMURF1 exosomal fraction were associated with GO functional annotation biological processes “extracellular matrix organization” and “ossification” (Supplementary Fig. 5).

Conditioned media from SMURF1-silenced cells reduces OVX-induced bone loss

We used an ovariectomized (OVX) mouse model to simulate osteoporosis in postmenopausal women, aiming to evaluate the influence of conditioned media (CM) from transfected cells on bone regeneration. To perform this analysis, it was first necessary to generate the experimental CMs in a mouse MSC line C3H10t1/2 where we are able to achieve efficient silencing of the *Smurf1* gene [22]. One week after the ovariectomy we conducted a one-time intramedullary injection in the femurs of the mice (Fig. 6A). Three groups of OVX mice were established: One was injected with NaCl (NaCl), one group was injected with CM from murine MSCs transfected with a control GapmeR (CM-Ctrl), and one with CM from cells transfected with a GapmeR targeting *Smurf1*

(CM-*Smurf1*). A control group where ovariectomy was not performed was also included in this experiment (No-OVX). (Fig. 6B).

Trabecular bone changes in the distal femur were analyzed using a micro-CT scan one month after injection (Fig. 6A). The NaCl-treated group exhibited a significant decline in trabecular bone showing bones almost depleted of trabecular structures compared to the NO-OVX mice. Importantly, mice injected with the CM-*Smurf1* showed a higher proportion of trabecular bone compared to both the OVX mice and CM-Ctrl groups (Fig. 6B).

Further analysis of micro-CT parameters revealed a significant increase in the Bone Volume to Total Volume (BV/TV) ratio in CM-*Smurf1* compared to both the OVX and CM-Ctrl, indicating a bone formation effect of *Smurf1* silencing on the pro-osteogenic activity of the CM. The positive effect of CM-*Smurf1* was also reflected in the trabecular number (Tb.N) and trabecular separation (Tb.sp) values, though no significant differences were observed at this level between the CM-Ctrl and CM-*Smurf1* groups (Fig. 6C). No significant differences in cortical bone parameters were observed between the different experimental groups (Supplementary Fig. 6).

Discussion

The significant increase in osteoporosis prevalence, coupled with the limitations and side effects of current pharmacological therapies, necessitates the development of new treatment strategies. New anabolic drugs such as Romosozumab have created great expectations in the field of osteoporosis due to its dual antiresorptive and osteoanabolic actions [32, 33]. Nevertheless, concerns remain with regards to the potential adverse effects of Romosozumab on endocrine and cardiovascular systems [34]. These concerns underscore the need for alternative treatment strategies that are both clinically safe and cost-effective.

MSCs secretome has been highlighted in recent years as a possible therapeutic approach for tissue regeneration [35]. However, since natural secretome might not

(See figure on next page.)

Fig. 5 Pro-osteogenic activity of the soluble (SF) and vesicular (VF) fractions of CM-SMURF1. **(A)** Top Panel. Expression of osteogenic markers, alkaline phosphatase activity and mineralization at day 16 of osteogenic differentiation after preconditioning with either the soluble (SF) or vesicular (VF) fractions of the hCM-SMURF1. *RUNX2* and *ALPL* expression, as well as alkaline phosphatase activity and mineralization show significant increases in SF of hCM-SMURF1 in relation to hCM-Ctrl. VF do not impact *RUNX2*, *ALPL* or alkaline phosphatase activity, however significant enhancement in mineralization is observed. Results are presented as means \pm SEM (*n* = 3). *: *p*-value < 0.05; **: *p*-value < 0.01; ***: *p*-value < 0.001. **(B)** Alizarin Red staining of representative samples reflecting the stimulation of mineralization in the SF and VF of hCM-SMURF1. **(C)** Volcano plot showing differently expressed proteins between hCM-Ctrl and hCM-SMURF1 for both SF and VF. Statistical significance was determined using an adjusted *t*-test against CM-Ctrl, with a *p*-value threshold of 0.05 and a fold change of 2 or greater. **(D)** Validation of relative expression by quantitative PCR of 2 genes overexpressed in soluble fraction (*SPARC* and *CCN2*) and 2 genes overexpressed in vesicular fraction (*PREPL* and *FMOD*) of CM-SMURF1. Results are presented as means \pm SEM. *: *p*-value < 0.05. (*n* = 5)

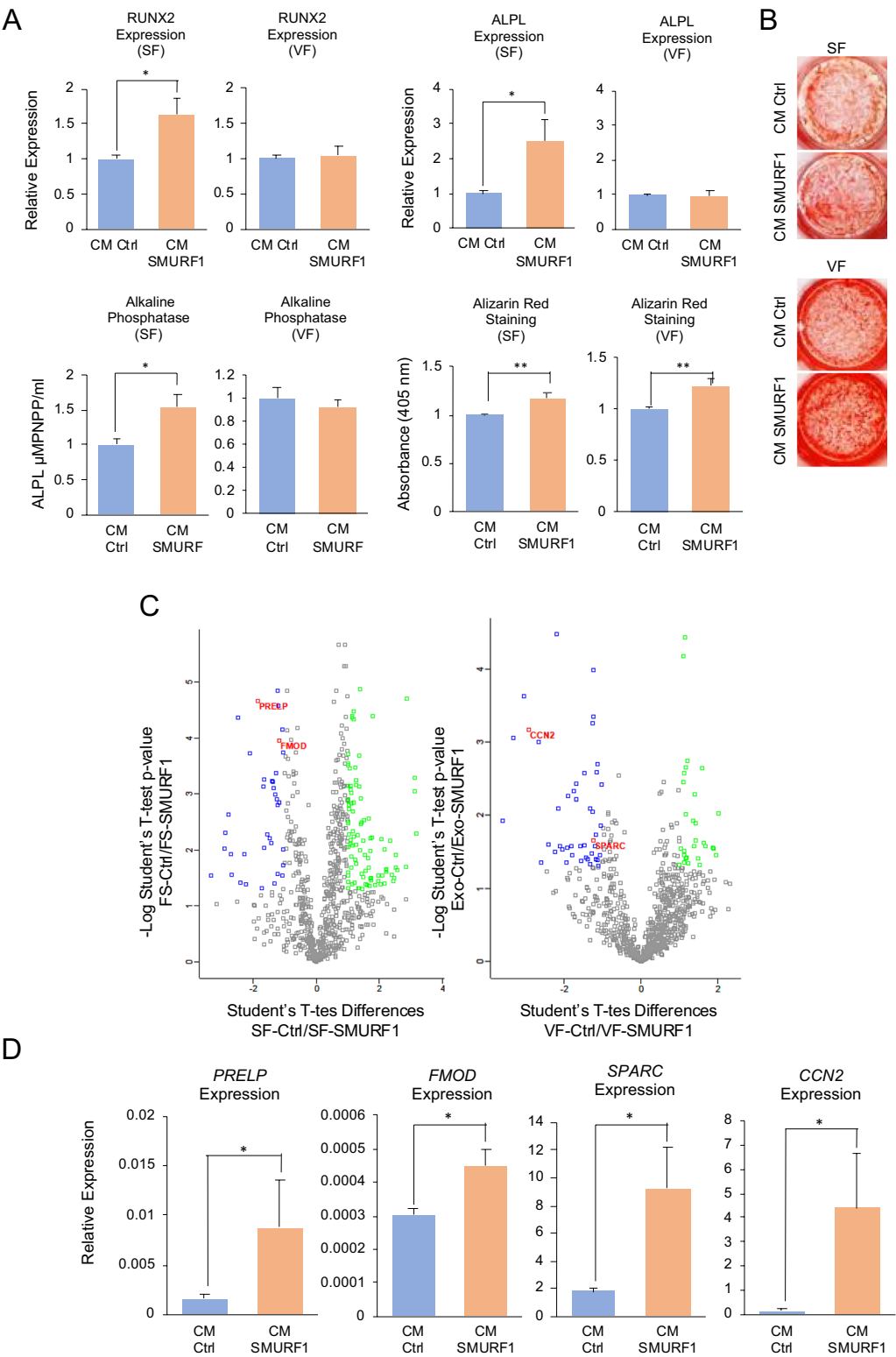


Fig. 5 (See legend on previous page.)

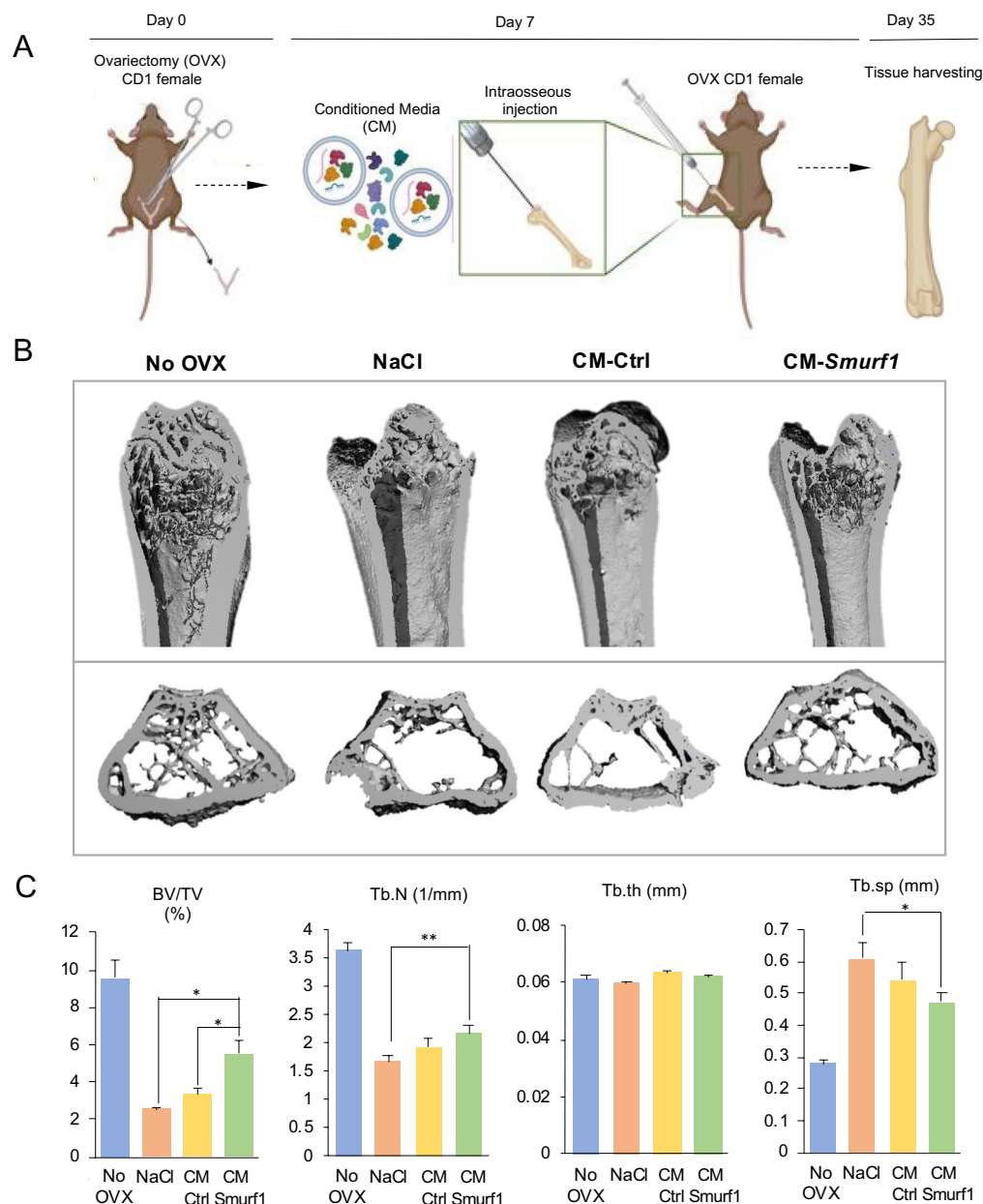


Fig. 6 MicroCT analysis of the osteo-regenerative effect of the local intraosseous administration of the CM-Smurf1 in a post-menopausal osteoporotic mouse model. **(A)** Experiment outline, **(B)** representative micro-CT coronal and trans-axial images femurs from Non-Ovariectomized mice (No-OVX), OVX mice treated with NaCl (NaCl), OVX mice treated with the CM-Ctrl (CM-Ctrl) and OVX mice treated with CM-Smurf1 (CM-Smurf1), **(C)** bone volume/tissue volume (BV/TV; %), trabecular number (Tb.N), trabecular thickness (Tb.Th) and space between trabecula were analyzed by using a Quantum GX micro-CT imaging system (PerkinElmer). Results are presented as means ± SEM (n = 5). *: p -value < 0.05; **: p -value < 0.01

be able to provide sufficient optimal regenerative effects in various disease conditions, secretome bioengineering is currently being explored. The plasticity of the MSCs secretome allows modulation of the composition of its different fractions (soluble and vesicular) to increase its osteo-regenerative potential. This enhancement can be

achieved by different means, including the suppression of anti-osteogenic proteins via genetic manipulation. Such intervention could lead to significant changes in the production of diverse bioactive molecules, resulting in a secretome that could positively influence the entire bone marrow microenvironment and promote bone formation.

Consequently, this optimized secretome would hold increased utility as a therapeutic tool.

This current study explores the potential of using the secretome from *SMURF1*-silenced MSCs as a novel therapeutic approach for osteoporosis. Previous works from our group have shown that transient silencing of *Smurf1*, a known BMP signaling inhibitor [36], in murine MSCs of osteoporotic animals leads to a significant increase in bone formation in vivo [24]. However, when *Smurf1* was silenced in murine MSCs in vitro prior to inducing osteogenic differentiation, the pro-osteogenic effect was significantly smaller and did not correspond with the substantial bone formation observed in vivo [22]. These results would suggest a key role of the paracrine action of the *SMURF1*-silenced MSCs in bone formation, aligning with previous studies that highlight that many of the regenerative effects of MSCs are due to their ability to empower tissue-resident cells through the secretion of trophic factors rather than to their intrinsic potential to differentiate into specific cell lines [37–39].

To further investigate the osteogenic potential of the secretome of cells where *SMURF1* has been silenced, we performed different in vitro analyses where rat primary MSCs and cells from the human cell line ASC52telo were respectively pre-treated with conditioned media (CM) from murine (CM-*Smurf1*) or human (hCM-*SMURF1*) cells where this gene had been previously silenced, prior to the induction of osteogenic differentiation. Our in vitro results clearly indicate that the CM from cells modified in this fashion enhances osteogenic differentiation, as evidenced by the significantly increased alkaline phosphatase (ALPL) activity and mineralization in rat primary MSCs pre-treated with the CM-*Smurf1*, and the increased mineralization in the ASC52telo hMSCs pre-treated with the hCM-*SMURF1*. Several studies have consistently shown that mineralization assays, such as alizarin red staining, provide the most conclusive evidence of functional osteogenesis [40, 41]. Although, except for the increase in *Alpl* expression in the murine system, none of the key osteogenic markers demonstrated statistically significant alterations in their expression levels, the enhanced mineral deposition after pretreatment of human or murine MSCs with the correspondent CM, serves as a definitive indicator of enhanced osteogenic differentiation in both systems. The marked effect of CM-*SMURF1* on bone regeneration in the ectopic rat model further supports these in vitro results, demonstrating the considerable bone-forming activity of the secretome from cells in which *SMURF1* has been silenced. Importantly, the increased mineralization of MSCs pre-treated with hCM-*SMURF1* also extends to primary MSCs isolated from osteoporotic patients (hOP-MSCs), characterized by an intrinsically reduced osteogenic potential

[27] proving the considerable osteo-inductive potential of hCM-*SMURF1* even under pathological conditions. This enhanced mineralization results replicated in all these different biological settings clearly increases the generalizability of the effects and their biological consistency, suggesting that the underlying biological mechanisms are evolutionally conserved. These results also highlight the crucial role of the BMP signaling pathway, highly conserved across diverse organisms [42], underscoring its potential as a target for medical interventions aimed to promote bone regeneration. It is also important to highlight that the osteogenic induction mediated by hCM-*SMURF1* seems to be as effective as BMP2 in promoting bone regeneration in hOP-MSCs in vitro. Although BMP2 is most commonly applied in surgical procedures for bone regeneration for its osteoinductive properties, its usefulness in promoting bone mineralization in vitro, provides us with a benchmark for evaluating the functional capacity of the hCM-*SMURF1* [43, 44]. The fact that CM-*SMURF1* is able to induce comparable levels of mineralization to those induced by BMP2, suggests that this CM-*SMURF1* possesses significant osteogenic capabilities.

Our study also confirms that CM from human MSCs with silenced *SMURF1* is non-cytotoxic and does not significantly affect cell proliferation and migration of MSCs, the latter being imperative for systemic tissue repair processes such as those compromised in osteoporosis. The increased chemotactic responses observed in cells pre-treated with CM-*SMURF1* might be of use for the functionalization of scaffolds to create a bone replacement material with intrinsic cell-attractive ability. The overall enhanced activity of all CM in wound healing assays implies potential benefits of all CM for bone regeneration. However, CM-*SMURF1* and CM-Ctrl-treated MSCs seem to be equally active in these processes. The fact that this secretome does not exhibit apparent cytotoxic effects opens the possibility for its clinical application. This non-cytotoxic nature is crucial, as it ensures the safety of using CM-*SMURF1* in therapeutic settings, potentially allowing for the development of novel treatments that leverage its osteo-inductive and chemotactic properties without adverse effects on cellular health.

Ex vivo bone cultures preserve the natural architecture and cellular interactions of the bone tissue, allowing for a more physiologically relevant environment compared to in vitro cultures of isolated bone marrow MSCs [45, 46]. In ex vivo cultures, the spatial organization, extracellular matrix composition, and interactions between various cell types—such as osteoblasts, osteoclasts, and stromal cells—mimic the in vivo setting more closely. This setup provides insights into how an agent affects bone formation within the context of the bone's natural

microenvironment, including the signaling pathways and cellular responses in a three-dimensional tissue context. Our ex vivo human bone culture analysis showed that incubation with a CM from MSCs transfected with a GapmeR specific for the silencing of *SMURF1*, resulted in a marked decrease in *RANKL* expression, a key molecule for osteoclast differentiation and activation, while the levels of osteoprotegerin (*OPG*), a decoy receptor that binds to *RANKL* preventing it from interacting with its receptor, remained unchanged. This led to a reduced *RANKL/OPG* ratio, indicating lower osteoclast activity and bone resorption, as a higher *OPG* level relative to *RANKL* means less stimulation for osteoclasts to mature and resorb bone [47, 48]. In this ex vivo context, the unchanged levels of M-CSF, a crucial factor for the survival and proliferation of osteoclast precursors, would suggest that the bioactive agent/s present in the secretome affecting *RANKL* do not interfere with the recruitment or survival of these osteoclast precursors. No significant change was either observed in the expression levels of *BGLAP*, a marker for osteoblasts activity, suggesting that osteoblast activity remains constant in this experimental setting. These findings highlight hCM-*SMURF1*'s potential as a targeted therapy for osteoporosis by inhibiting osteoclast activity and bone resorption. The effectiveness of hCM-*SMURF1* in reducing *RANKL* levels would make it a promising candidate for further in vivo studies and clinical trials aimed at treating bone resorption disorders.

These results from the in vivo analysis performed through an intraosseous injection in the femur of a postmenopausal osteoporotic mouse model would indicate that the CM from *Smurf1*-silenced cells (CM-*Smurf1*) significantly enhances bone regeneration and density in osteoporotic conditions induced by OVX. The bone structure in the CM-*Smurf1* group closely approximates that of the No-OVX group, suggesting its potential efficacy in treating osteoporosis. Notably, these results were achieved after a single injection of CM-*Smurf1*, suggesting that extended treatment could further prevent bone loss. This finding underscores the potent effect of the secretome from *Smurf1*-silenced MSCs, promoting bone formation and reducing bone loss more effectively than the control conditioned media. These observations support the hypothesis that *Smurf1*-silenced MSC-derived secretome can enhance bone regeneration and may serve as a promising therapeutic approach for osteoporosis.

We isolated the soluble and vesicular fractions of the secretome of ASC52telo cells where *SMURF1* has been silenced, and analyzed their osteogenic effects separately to allow for the identification of specific bioactive components and their mechanisms of action. The results indicate that the soluble fraction (SF) of CM-*SMURF1*

significantly enhances the expression of *Runx2* compared to the vesicular fraction (VF). *Runx2* serves as a master gene that orchestrates the expression of other osteogenic genes [49]. The elevated expression of *Runx2* in response to SF treatment suggests that the soluble components of the secretome play a more pivotal role in initiating osteogenesis. Similarly, the expression of *ALPL*, which encodes alkaline phosphatase, is also markedly increased in cells treated with the SF compared to those treated with the VF. Despite these differences at the level of induction of osteogenic genes, both fractions seem to promote similar levels of in vitro mineralization. While the upregulation of osteogenic markers such as *RUNX2* and *ALPL* is crucial for the initial stages of osteoblast differentiation, mineralization is a multifaceted process that involves not only gene expression but also the deposition of the extracellular matrix and subsequent mineral deposits. This mineralization process is not solely dependent on the expression of osteogenic genes but also on the functional activities of various enzymes and matrix proteins. Extracellular vesicles can enhance mineralization by providing necessary components and signals that promote or catalyze the deposition of mineral content within the extracellular matrix, a key step in bone formation [50, 51]. In summary, the vesicular fraction (VF) likely promotes mineralization through mechanisms that involve direct enhancement of mineral deposition, provision of osteoinductive components, and modulation of the extracellular environment, which together complement the early osteogenic gene expression induced by the soluble fraction (SF). These combined effects result in similar levels of mineralization observed in vitro, despite differences in early gene expression and enzyme activity.

To further elucidate the mechanisms by which the SF and VF impart their pro-osteogenic effects, mass spectrometry analysis of the two fractions was conducted. For each of the fractions we performed a gene ontology (GO) analysis of proteins differentially represented in the Ctrl and *SMURF1*-silenced samples, using a *p*-value threshold of 0.05 and a fold change of 2 or greater. This analysis identified functions that can be associated with regeneration processes such as “regulation of cell morphogenesis” or “post-transcriptional regulation of gene expression” in the soluble fraction of CM-*SMURF1* whereas functions suggesting a positive switch towards pro-osteogenic functions such as “extracellular matrix organization” or “ossification” are enriched in vesicular fraction of CM-*SMURF1*. Some of the factors identified in the soluble and vesicular fractions of the CM-*SMURF1*, whose differential expression was validated by qPCR, play important roles in bone formation. *SPARC* (Secreted Protein Acidic and Cysteine Rich) is crucial for bone mineralization, influencing the deposition of minerals within the

bone matrix. It interacts with extracellular matrix components and growth factors, enhancing osteoblast proliferation and differentiation [52, 53]. On the other hand, *CCN2* (Cellular Communication Network Factor 2), is also crucial for osteogenesis. It promotes osteoblast differentiation and bone matrix production by interacting with key signaling pathways such as TGF- β , BMPs, and Wnt [54]. *CCN2* enhances the maturation and activity of osteoblasts, which are essential for bone formation. It binds to TGF- β and BMPs, enhancing their signaling and promoting bone matrix production [55]. Furthermore, *CCN2* has multiple domains that enable it to interact with various proteins in the extracellular matrix (ECM), facilitating complex signaling necessary for bone development [56].

Overall, the engineered secretome from *SMURF1*-silenced MSCs showcases important osteogenic potential, presenting a compelling opportunity for clinical translation in osteoporosis treatment. While scaling up the production of MSC-derived secretome to industrial levels involves significant challenges, advancements in bioreactor technology, standardization protocols, and regulatory frameworks provide a feasible path forward. By addressing issues related to cell expansion, consistency, isolation, and compliance, large-scale production can be achieved. The non-cytotoxic nature of this secretome and its ability to enhance mineralization in MSCs from osteoporotic patients highlight its potential as a safe and effective therapeutic tool. This novel approach could provide a significant advancement in the treatment of osteoporosis, offering a promising alternative to current pharmacological therapies.

Conclusion

In conclusion, our findings demonstrate that the secretome from *SMURF1*-silenced MSCs significantly enhances osteogenic potential, offering a promising therapeutic approach for osteoporosis. Both the soluble and vesicular fractions contribute to improved mineralization and osteogenic differentiation. Mass spectrometry and gene ontology analyses identified key regenerative pathways, while in vivo studies confirmed the substantial bone-forming activity of the secretome. Importantly, the pro-osteogenic potential was also proven in primary cells from osteoporotic patients, highlighting its relevance in pathological conditions. This novel, non-cytotoxic, and effective treatment could revolutionize osteoporosis management, providing a safe and cost-effective alternative to current therapies.

Supplementary Information

The online version contains supplementary material available at <https://doi.org/10.1186/s13287-025-04165-0>.

Additional file 1.
Additional file 2.
Additional file 3.
Additional file 4.
Additional file 5.

Acknowledgements

During the preparation of this work, the author(s) used an AI language model (ChatGPT) to ensure grammatical accuracy in the English language text. After using this tool, the author(s) reviewed and edited the content as needed and take(s) full responsibility for the content of the published article.

Author contributions

Alberto González-González, Itziar Álvarez-Iglesias and Daniel García-Sánchez, molecular laboratory work and manuscript preparation. Ricardo Reyes Histology analysis. Ana Alfonso-Fernández Postmenopausal osteoporosis mouse model, intraosseous injection, and financial support. Alfonso Bolado proteomic analysis. Patricia Díaz-Rodríguez characterization of extracellular vesicles (TEM and NTA). María Isabel Pérez-Núñez, sourcing of human osteoporotic bone samples. José Carlos Rodríguez-Rey financial support. Jesús Delgado-Calle financial support and study conceptualization and Flor M. Pérez-Campo financial support, study conceptualization and manuscript preparation.

Funding

The authors acknowledge funding by a grant from the Spanish Ministerio de Economía y Competitividad (Project PID2021-127493OB-C21), one grant from the Instituto de Salud Carlos III (PI22/0264) and two grants from the National Institutes of Health (R37-CA251763, R01-CA209882) to Jesús Delgado-Calle. Alberto González-González and Daniel García-Sánchez were funded by two grants from the Instituto de Investigación Marqués de Valdecilla-IDIVAL (PREVAL19/02 and PREVAL 20/01). Itziar Álvarez-Iglesias was funded by a project from the Instituto de Investigación Marqués de Valdecilla (NVAL 23/06). We extend our gratitude to the Boehringer Ingelheim Fonds for partially support three months stay of Alberto González-González in the laboratory of Dr. Jesús Delgado-Calle (University of Arkansas).

Availability of data and materials

The datasets used and/or analyzed during the current study are included in the manuscript (Supplementary Tables 1 and 2).

Declarations

Ethics approval and consent to participate

The study was conducted according to the guidelines of the Declaration of Helsinki. This study was approved by the Institutional Bioethics Committee of the University of Cantabria (Reference 2015/21; Project Title: Enhancing Mesenchymal Stem Cells Osteogenic Capacity Through Modulation of the Bone Marrow Microenvironment; date of approval 04–11–22) and the Consejería de Agricultura y Ganadería de Cantabria (Reference PI-08–21; Project Title: Modulation of the Regenerative Capacity of Mesenchymal Stem Cells for Their Use in Therapies Applied to the Musculoskeletal System; date of approval 01–11–21). Bone samples were obtained from the patients after anonymization. Informed consent was obtained from all the subjects involved in the study.

Consent for publication

Not applicable.

Competing interests

The authors declare that they have no competing interests.

Author details

¹Department of Biochemistry and Molecular Biology, Faculty of Medicine, University of Cantabria-IDIVAL, 39012 Santander, Spain. ²Department of Physiology and Cell Biology, Winthrop P. Rockefeller Cancer Institute, University of Arkansas for Medical Sciences, Little Rock, AR 72205, USA. ³Department of Biochemistry, Microbiology, Cell Biology and Genetics, Universidad de La Laguna, 38206 La Laguna, Spain. ⁴Department of Traumatology, Hospital Universitario Marqués de Valdecilla, University of Cantabria, 39008 Santander, Spain. ⁵I+D Farma Group (GI-1645), Department of Pharmacology, Pharmacy and Pharmaceutical Technology, Facultad de Farmacia, Instituto de Materiales (IMATUS) and Health Research Institute of Santiago de Compostela (IDIS), Universidad de Santiago de Compostela, 15782 Santiago de Compostela, Spain. ⁶Cancer Research UK Scotland Centre, Institute of Genetics and Cancer, University of Edinburgh, Edinburgh EH4 2XR, UK.

Received: 25 October 2024 Accepted: 21 January 2025

Published online: 07 February 2025

References

- Yadav VK, Balaji S, Suresh PS, Liu XS, Lu X, Li Z, Guo XE, Mann JJ, Balapure AK, Gershon MD, Medhamurthy R, Vidal M, Karsenty G, Ducey P. Pharmacological inhibition of gut-derived serotonin synthesis is a potential bone anabolic treatment for osteoporosis. *Nat Med*. 2010;16(3):308–12.
- Khosla S, Riggs BL. Pathophysiology of age-related bone loss and osteoporosis. *Endocrinol Metab Clin North Am*. 2005;34(4):1015–30.
- Simpson ER. Sources of estrogen and their importance. *J Steroid Biochem Mol Biol*. 2003;86(3–5):225–30.
- Riggs BL, Melton LJ 3rd. The prevention and treatment of osteoporosis. *N Engl J Med*. 1992;327(9):620–7.
- Skjold MK, Frost M, Abrahamsen B. Side effects of drugs for osteoporosis and metastatic bone disease. *Br J Clin Pharmacol*. 2019;85(6):1063–71.
- Ocarino NM, Boeloni JN, Jorgetti V, Gomes DA, Goes AM, Serakides R. Intra-bone marrow injection of mesenchymal stem cells improves the femur bone mass of osteoporotic female rats. *Connect Tissue Res*. 2010;51(6):426–33.
- Uejima S, Okada K, Kagami H, Taguchi A, Ueda M. Bone marrow stromal cell therapy improves femoral bone mineral density and mechanical strength in ovariectomized rats. *Cytotherapy*. 2008;10(5):479–89.
- Yu Z, Zhu T, Li C, Shi X, Liu X, Yang X, Sun H. Improvement of intertrochanteric bone quality in osteoporotic female rats after injection of polylactic acid-polyglycolic acid copolymer/collagen type I microspheres combined with bone mesenchymal stem cells. *Int Orthop*. 2012;36(10):2163–71.
- Liu Y, Wang L, Liu S, Liu D, Chen C, Xu X, Chen X, Shi S. Transplantation of SHED prevents bone loss in the early phase of ovariectomy-induced osteoporosis. *J Dent Res*. 2014;93(11):124–32.
- Sui BD, Hu CH, Zheng CX, Shuai Y, He XN, Gao PP, Zhao P, Li M, Zhang XY, He T, Xuan K, Jin Y. Recipient glycemic micro-environments govern therapeutic effects of mesenchymal stem cell infusion on osteopenia. *Theranostics*. 2017;7(5):1225–44.
- Han Y, Yang J, Fang J, Zhou Y, Candi E, Wang J, Hua D, Shao C, Shi Y. The secretion profile of mesenchymal stem cells and potential applications in treating human diseases. *Signal Transduct Target Ther*. 2022;7(1):92.
- Liang X, Ding Y, Zhang Y, Tse HF, Lian Q. Paracrine mechanisms of mesenchymal stem cell-based therapy: current status and perspectives. *Cell Transplant*. 2014;23(9):1045–59.
- Cheung WH, Miclau T, Chow SK, Yang FF, Alt V. Fracture healing in osteoporotic bone. *Injury*. 2016;47(Suppl 2):S21–26.
- Park D, Spencer JA, Koh BI, Kobayashi T, Fujisaki J, Clemens TL, Lin CP, Kronenberg HM, Scadden DT. Endogenous bone marrow MSCs are dynamic, fate-restricted participants in bone maintenance and regeneration. *Cell Stem Cell*. 2012;10(3):259–72.
- Caplan AI, Correa D. The MSC: an injury drugstore. *Cell Stem Cell*. 2011;9(1):11–5.
- Murphy MB, Moncivais K, Caplan AI. Mesenchymal stem cells: environmentally responsive therapeutics for regenerative medicine. *Exp Mol Med*. 2013;45(11):e54.
- Catalano A, Loddo S, Bellone F, Pecora C, Lasco A, Morabito N. Pulsed electromagnetic fields modulate bone metabolism via RANKL/OPG and Wnt/beta-catenin pathways in women with postmenopausal osteoporosis: a pilot study. *Bone*. 2018;116:42–6.
- Huang TB, Li YZ, Yu K, Yu Z, Wang Y, Jiang ZW, Wang HM, Yang GL. Effect of the Wnt signal-RANKL/OPG axis on the enhanced osteogenic integration of a lithium incorporated surface. *Biomater Sci*. 2019;7(3):1101–16.
- Man K, Brunet MY, Fernandez-Rhodes M, Williams S, Heaney LM, Gethings LA, Federici A, Davies OG, Hoey D, Cox SC. Epigenetic reprogramming enhances the therapeutic efficacy of osteoblast-derived extracellular vesicles to promote human bone marrow stem cell osteogenic differentiation. *J Extracell Vesicles*. 2021;10(9):e12118.
- Zhang X, Zhao Q, Zhou N, Liu Y, Qin K, Buhl EM, Wang X, Hildebrand F, Balmayor ER, Greven J. Osteoblast derived extracellular vesicles induced by dexamethasone: a novel biomimetic tool for enhancing osteogenesis in vitro. *Front Bioeng Biotechnol*. 2023;11:1160703.
- García-García P, Ruiz M, Reyes R, Delgado A, Évora C, Riancho JA, Rodríguez-Rey JC, Pérez-Campo FM. Smurf1 silencing using a LNA-ASOs/lipid nanoparticle system to promote bone regeneration. *Stem Cells Transl Med*. 2019;8(12):1306–17.
- García-Sánchez D, González-González A, García-García P, Reyes R, Pérez-Núñez MI, Riancho JA, Évora C, Rodríguez-Rey JC, Pérez-Campo FM. Effective osteogenic priming of mesenchymal stem cells through LNA-ASOs-mediated Sfrp1 gene silencing. *Pharmaceutics*. 2021;13(8):1277.
- García-García P, Reyes R, García-Sánchez D, Pérez-Campo FM, Rodríguez-Rey JC, Évora C, Díaz-Rodríguez P, Delgado A. Nanoparticle-mediated selective Sfrp-1 silencing enhances bone density in osteoporotic mice. *J Nanobiotechnol*. 2022;20(1):462.
- García-García P, Ruiz M, Reyes R, Delgado A, Évora C, Riancho JA, Rodríguez-Rey JC, Pérez-Campo FM. Smurf1 silencing using a LNA-ASOs/lipid nanoparticle system to promote bone regeneration. *Stem Cells Transl Med*. 2019;8(12):1306–17.
- Rodríguez-Evora M, García-Pizarro E, del Rosario C, Pérez-López J, Reyes R, Delgado A, Rodríguez-Rey JC, Évora C. Smurf1 knocked-down, mesenchymal stem cells and BMP-2 in an electrosensory system for bone regeneration. *Biomacromol*. 2014;15(4):1311–22.
- Fañan-Labora J, Fernández-Pernas P, Fuentes I, De Toro J, Oreiro N, Sangiao-Alvarellos S, Mateos J, Arufe MC. Influence of age on rat bone-marrow mesenchymal stem cells potential. *Sci Rep*. 2015;5:16765.
- Del Real A, Pérez-Campo FM, Fernández AF, Sanudo C, Ibarbia CG, Pérez-Núñez MI, Crikkinge WV, Braspenning M, Alonso MA, Fraga MF, Riancho JA. Differential analysis of genome-wide methylation and gene expression in mesenchymal stem cells of patients with fractures and osteoarthritis. *Epigenet: Off J DNA Methylation Soc*. 2017;12(2):113–22.
- Delgado-Calle J, Sanudo C, Sánchez-Verde L, García-Renedo RJ, Arozamena J, Riancho JA. Epigenetic regulation of alkaline phosphatase in human cells of the osteoblastic lineage. *Bone*. 2011;49(4):830–8.
- Gregory CA, Gunn WG, Peister A, Prockop DJ. An Alizarin red-based assay of mineralization by adherent cells in culture: comparison with cetylpyridinium chloride extraction. *Anal Biochem*. 2004;329(1):77–84.
- García-Sánchez D, González-González A, Álvarez-Iglesias I, Dujo-Gutiérrez MD, Bolado-Carrancio A, Certo M, Pérez-Núñez MI, Riancho JA, Rodríguez-Rey JC, Delgado-Calle J, Pérez-Campo FM. Engineering a pro-osteogenic secretome through the transient silencing of the gene encoding secreted frizzled related protein 1. *Int J Mol Sci*. 2023;24(15):5825.
- Garmilla-Ezquerria P, Sanudo C, Delgado-Calle J, Pérez-Núñez MI, Sumilera M, Riancho JA. Analysis of the bone microRNome in osteoporotic fractures. *Calcif Tissue Int*. 2015;96(1):30–7.
- Saag KG, Petersen J, Brandt ML, Karaplis AC, Lorentzon M, Thomas T, Maddox J, Fan M, Meisner PD, Grauer A. Romosozumab or alendronate for fracture prevention in women with osteoporosis. *N Engl J Med*. 2017;377(15):1417–27.
- Mineta K, Nishisho T, Okada M, Kamada M, Sairyo K. Real-world effects, safety, and predictors of the effectiveness of romosozumab in primary and secondary osteoporosis: an observational study. *Bone*. 2024;186:117164.
- Cosman F, Crittenden DB, Adachi JD, Binkley N, Czerwinski E, Ferrari S, Hofbauer LC, Lau E, Lewiecki EM, Miyauchi A, Zerbini CA, Milmont CE, Chen L, Maddox J, Meisner PD, Libanati C, Grauer A. romosozumab treatment in postmenopausal women with osteoporosis. *N Engl J Med*. 2016;375(16):1532–43.

35. Trigo CM, Rodrigues JS, Camoes SP, Sola S, Miranda JP. Mesenchymal stem cell secretome for regenerative medicine: where do we stand?. *J Adv Res*. 2024. <https://doi.org/10.1016/j.jare.2024.05.004>.
36. Shimazu J, Wei J, Karsenty G. Smurf1 inhibits osteoblast differentiation, bone formation, and glucose homeostasis through serine 148. *Cell Rep*. 2016;15(1):27–35.
37. Marques CR, Marote A, Mendes-Pinheiro B, Teixeira FG, Salgado AJ. Cell secretome based approaches in Parkinson's disease regenerative medicine. *Expert Opin Biol Ther*. 2018;18(12):1235–45.
38. Miranda JP, Camoes SP, Gaspar MM, Rodrigues JS, Carvalheiro M, Barcia RN, Cruz P, Cruz H, Simoes S, Santos JM. The secretome derived from 3D-cultured umbilical cord tissue mscs counteracts manifestations typifying rheumatoid arthritis. *Front Immunol*. 2019;10:18.
39. Noronha NC, Mizukami A, Caliar-Oliveira C, Cominal JG, Rocha JLM, Covas DT, Swiech K, Malmegrim KCR. Priming approaches to improve the efficacy of mesenchymal stromal cell-based therapies. *Stem Cell Res Ther*. 2019;10(1):131.
40. Serguenco A, Wang MY, Myklebost O. Real-time vital mineralization detection and quantification during in vitro osteoblast differentiation. *Biol Proced Online*. 2018;20:14.
41. Moester MJ, Schoeman MA, Oudshoorn IB, van Beusekom MM, Mol IM, Kaijzel EL, Lowik CW, de Rooij KE. Validation of a simple and fast method to quantify in vitro mineralization with fluorescent probes used in molecular imaging of bone. *Biochem Biophys Res Commun*. 2014;443(1):80–5.
42. Akiyama T, Raftery LA, Wharton KA. Bone morphogenetic protein signaling: the pathway and its regulation. *Genetics*. 2024;226(2):iyad200.
43. Scarfi S. Use of bone morphogenetic proteins in mesenchymal stem cell stimulation of cartilage and bone repair. *World J Stem Cells*. 2016;8(1):1–12.
44. Bez M, Pelled G, Gazit D. BMP gene delivery for skeletal tissue regeneration. *Bone*. 2020;137: 115449.
45. Bellido T, Delgado-Calle J. Ex vivo organ cultures as models to study bone biology. *JBMR Plus*. 2020;4(3):e10345.
46. Cramer EEA, Ito K, Hofmann S. Ex vivo bone models and their potential in preclinical evaluation. *Curr Osteoporos Rep*. 2021;19(1):75–87.
47. Theoleyre S, Wittrant Y, Tat SK, Fortun Y, Redini F, Heymann D. The molecular triad OPG/RANK/RANKL: involvement in the orchestration of pathophysiological bone remodeling. *Cytokine Growth Factor Rev*. 2004;15(6):457–75.
48. Wright HL, McCarthy HS, Middleton J, Marshall MJ. RANK, RANKL and osteoprotegerin in bone biology and disease. *Curr Rev Musculoskelet Med*. 2009;2(1):56–64.
49. Komori T. Regulation of osteoblast differentiation by Runx2. *Adv Exp Med Biol*. 2010;658:43–9.
50. Anderson HC. Matrix vesicles and calcification. *Curr Rheumatol Rep*. 2003;5(3):222–6.
51. Tkach M, Thery C. Communication by extracellular vesicles: where we are and where we need to go. *Cell*. 2016;164(6):1226–32.
52. Tsukasaki M, Takayanagi H. Osteoimmunology: evolving concepts in bone-immune interactions in health and disease. *Nat Rev Immunol*. 2019;19(10):626–42.
53. Zhang L, et al. Multistage genome-wide association meta-analyses identified two new loci for bone mineral density. *Hum Mol Genet*. 2014;23(7):1923–33.
54. Kubota S, Takigawa M. Role of CCN2/CTGF/Hcs24 in bone growth. *Int Rev Cytol*. 2007;257:1–41.
55. Abreu JG, Ketpura NI, Reversade B, De Robertis EM. Connective-tissue growth factor (CTGF) modulates cell signalling by BMP and TGF-beta. *Nat Cell Biol*. 2002;4(8):599–604.
56. Leask A, Abraham DJ. All in the CCN family: essential matricellular signaling modulators emerge from the bunker. *J Cell Sci*. 2006;119(Pt 23):4803–10.

Publisher's Note

Springer Nature remains neutral with regard to jurisdictional claims in published maps and institutional affiliations.